Journal of Low Temperature Physics, Vol. 2, No. 3/4, 1970

Classical Scattering of a Sphere by a Vortex— A Possible Explanation of the Steyert–Taylor–Kitchens Experiment*

William J. Titus

School of Physics and Astronomy
University of Minnesota, Minneapolis, Minnesota

(Received November 19, 1969)

A classical model for the scattering of a small particle by a rectilinear vortex in liquid He II is studied for the purpose of explaining the experimental results of Steyert, Taylor, and Kitchens. Although many of their observations are accounted for, verification of the theory would require a re-analysis of the experimental data. A classical analogue of an Iordanskii force is also discussed.

1. INTRODUCTION

In 1965, Steyert, Taylor, and Kitchens (STK)[1] reported an experiment where solid particles (frozen mixture of H-D gas) were injected into liquid He II ($1.4°K < T < 2.0°K$). Under a variety of flow conditions for the liquid, about one particle in a thousand was observed to undergo closed-loop motion (see Fig. 1). The diameter D and period T of the particle orbit were measured by photographic techniques. The orbiting motion was interpreted as a particle moving with the superfluid about a rectilinear vortex of circulation κ. Assuming the orbit is circular,

$$\kappa = \pi^2 D^2/T \tag{1}$$

With Eq. (1) and a statistical analysis of the resulting data, various values for κ were determined and found to be consistent with the quantized result $\kappa = nh/m_4$; here h is Planck's constant, m_4 is the mass of a He^4 atom, and n is a positive integer. However, a value of $n = \frac{1}{2}$ was also found for flow conditions arising from heat currents.

It is the purpose of this article to point out that an alternate interpretation of the experimental results may be obtained by assuming the loop motion is a result of the classical scattering of a small particle from a rectilinear vortex where viscous forces are neglected. Indeed some aspects of this problem were studied by Lord Kelvin in 1873.[2] He found that the force on the particle varied as r^{-3} for distances far from the vortex axis [(r, ϕ, z) will denote the cylindrical components of a radius

*Work partially supported by the U. S. Atomic Energy Commission under contract No. AT(11-1)-1569.

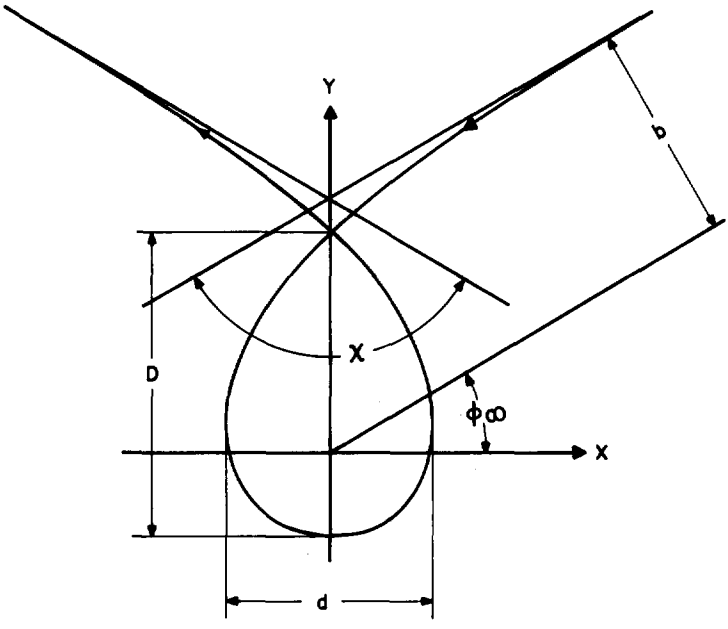

Fig. 1. A typical single-loop trajectory for a particle projected on the plane perpendicular to the vortex axis. The relevant parameters for the closed orbit are the width d, length D, closure time T, and area A. The value of the incident angle ϕ_∞ depends on the orientation of the x-axis; in this figure, the axis is chosen so that the angle of closest approach occurs at $\frac{3}{2}\pi$. The scattering angle $0 \leq \chi < 2\pi$ is defined counterclockwise from the incident direction. The quantity b is the impact parameter for a particle with radial velocity v_r at infinity.

vector with origin on the vortex axis and z-axis in the direction of vortex vorticity]; an actual plot of a single-loop orbit appears in his work. More recently, Fetter[3] investigated the scattering problem for the long-range force limit and showed that multiloop scattering is possible for certain particle velocities and impact parameters. The force $\mathbf{F}$ on the particle was calculated by an integration of the fluid pressure P over the particle surface σ, assuming the particle was at rest in the fluid. The pressure was related to the fluid velocity $\mathbf{v}$ and fluid density ρ_s by Bernoulli's theorem[4]

$$P = -\tfrac{1}{2}\rho_s \mathbf{v}^2 \tag{2}$$

For the long-range force behavior, $\mathbf{v}$ was approximated by the fluid velocity $\mathbf{v}_s$ in the absence of the particle; that is,

$$\mathbf{v}_s = (\kappa/r)\hat{\phi} \tag{3}$$

where $\kappa = (2\pi)^{-1}\kappa$. With these approximations, one finds

$$\mathbf{F} = -\int_\sigma P\, d\mathbf{S} = -\int \nabla P\, d^3R \approx \nabla(\tfrac{1}{2}\rho_s \mathbf{v}_s^2)V^* \tag{4}$$

The quantity V^* is an undetermined, effective particle volume.† Equation (4) gives a force proportional to r^{-3}. The scattering was then investigated using Eqs. (3) and (4) and the usual techniques of classical scattering theory. The results neglect fluid distortion around the particle, possible forces arising from the particle motion, and yield only long-range force behavior.

In this article, the classical problem is studied in more detail. In Section 2, the model considered is a spherical particle in an incompressible ideal fluid (He II at $T = 0$), where the fluid is undergoing rectilinear vortex motion of circulation κ. The simplifying assumption is made that the particle can never penetrate an infinitesimal region occupied by the vortex core; detailed structure of the vortex core is thus neglected. The velocity potential, the fluid kinetic energy, and the force on the particle are found. The force is calculated by an integration of the fluid pressure over the particle surface, as well as by a Hamiltonian formulation found in Lamb's book on hydrodynamics.[6] Aside from inertial effects, the force is the negative gradient of the fluid kinetic energy calculated when the particle is at rest. A simple extension is made to nonzero temperatures by assuming the only effect of viscosity is a renormalization of the particle mass. In Section 3, the scattering problem is solved for the case where the particle radius is small compared to the closest distance the particle approaches the center of the vortex; this approximation is consistent with the experimental work of STK. The results for one-loop orbits are considered in Section 4; an equation similar to (1), but modified by a factor depending on the shape of the particle orbit, is found relating κ, T, and D. Transport cross sections are given in Section 5 for the purpose of discussing a classical analogue of an Iordanskii force.[7]

2. IDEALIZED MODEL

Consider a spherical particle [mass m, radius a, and velocity $\mathbf{v}_p(t)$] in an infinite, incompressible ideal fluid of density ρ_s (He II at $T = 0$).‡ The fluid is undergoing rectilinear vortex motion of circulation κ. The particle and fluid are restricted to the region outside an infinitesimal vortex core of radius ε. By introducing an appropriate mathematical barrier, the fluid is irrotational throughout its domain; the fluid velocity $\mathbf{v}$ is then the negative gradient of a single-valued velocity potential Φ that satisfies Laplace's equation. The circulation condition requires that Φ differs by an amount κ on each side of the barrier. The boundary conditions on Φ are that $\nabla\Phi$ approaches zero at distances far from the vortex core and that the normal components of $\nabla\Phi$ and $-\mathbf{v}_p(t)$ are equal on the particle surface. The pressure P is related to Φ through Bernoulli's theorem

$$P = -\tfrac{1}{2}\rho_s \nabla\Phi\cdot\nabla\Phi + \rho_s\,\partial\Phi/\partial t + \rho_s\,c(t) \tag{5}$$

where $c(t)$ is spatially independent. The fluid kinetic energy T is given by

$$T = \tfrac{1}{2}\rho_s \int \nabla\Phi\cdot\nabla\Phi\, d^3R \tag{6}$$

†Donnelly[5] predicts that V^* is 3/2 the particle volume when the particle is a sphere.
‡The elementary results for classical hydrodynamics used in this article can be found in Ref. 4.

The fluid force **F** on the particle is

$$\mathbf{F} = -\int_{\sigma} P \, d\mathbf{S} \tag{7}$$

where σ is the spherical surface of the particle.

To determine Φ and its related quantities, the following geometry is used (see Fig. 2). At time t, when the particle has velocity $\mathbf{v}_p(t)$, two coordinate systems are chosen for descriptional purposes: the first (r_1, ϕ_1, z_1) is fixed on the vortex while the second (R_2, θ_2, ϕ_2) is located at the center of the particle. The cartesian axes of the two systems are parallel with the z-axes parallel to the vortex axis $\hat{\kappa}$. A barrier is placed in the plane $x_1 \leq -\varepsilon$, $y_1 = 0$. The fluid and particle are restricted from entering a vortex core region of radius ε.

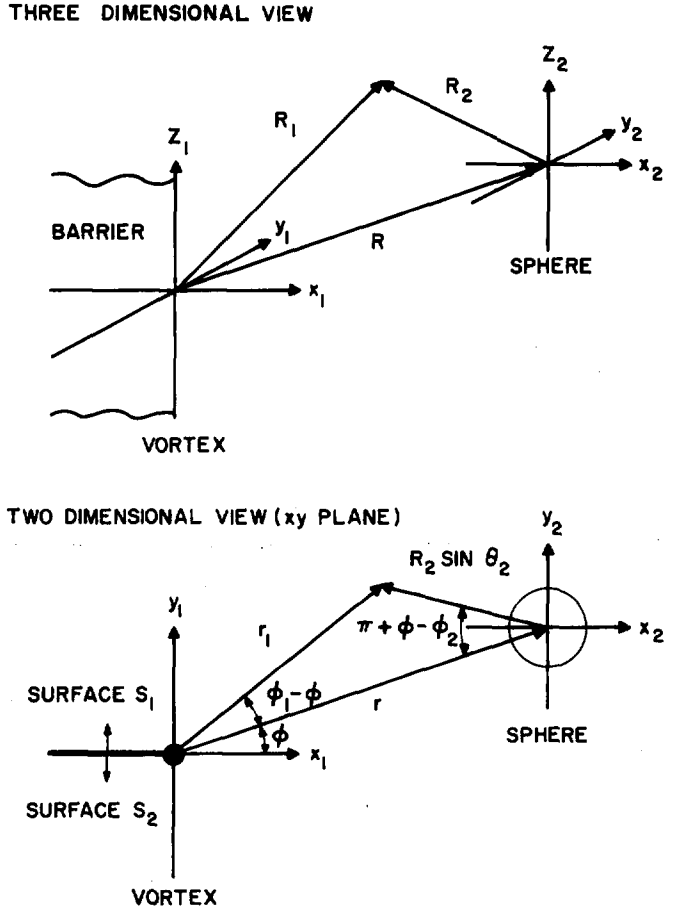

Fig. 2. The coordinate systems and vector notations used in the calculation of the velocity potential, the fluid kinetic energy, and the particle force.

The velocity potential Φ can be decomposed into Φ_p and Φ_v, where Φ_p is the velocity potential for a sphere in the absence of the vortex and Φ_v is the velocity potential for a stationary sphere in the presence of the vortex. In addition, Φ_v is the sum of Φ_0, the velocity potential of a vortex in the absence of the sphere and Ψ, a velocity potential expansible in spherical harmonics. In particular,†

$$\Phi_p = \tfrac{1}{2}(\mathbf{v}_p \cdot \mathbf{R}_2)(a/R_2)^3 \tag{8}$$

$$\Psi = -\kappa \sum_{lm} B_{lm} Y_{lm}(\theta_2, \phi')(a/R_2)^{l+1} \tag{9}$$

$$\begin{aligned} \Phi_0 &= -\kappa\phi' = -\kappa \arctan[\eta \sin\phi' (1 + \eta\cos\phi')^{-1}] \\ &= -\kappa \sum_{lm} C_{lm} Y_{lm}(\theta_2, \phi')(R_2/r)^l, \qquad \eta \leq 1 \end{aligned} \tag{10}$$

where

$$\phi' = \phi_2 - \phi, \qquad \eta = R_2 \sin\theta_2/r \tag{11}$$

$$C_{lm} = i2^{l-1}\Gamma(l)[4\pi/\Gamma(2 + 2l)]^{1/2}[\delta_{l,m} - (-1)^l\delta_{l,-m}] \tag{12}$$

The summation indices extend from $-l \leq m \leq l$ and $1 \leq l \leq \infty$. The constant B_{lm} is determined from the kinematical boundary condition

$$R_2 \partial\Phi/\partial R_2|_{R_2=a} = -(\mathbf{v}_p \cdot \mathbf{a}) \tag{13}$$

and is given by

$$B_{lm} = l(l + 1)^{-1} C_{lm}(a/r)^l \tag{14}$$

The velocity potential Ψ is then

$$\begin{aligned} \Psi &= -\kappa(a/R_2) \sum_{l=1}^{\infty} \eta'^l (-1)^{l+1}(l + 1)^{-1} \sin l\phi' \\ &= \kappa(r/a)\csc\theta_2 \{\cos\phi' \arctan[\eta' \sin\phi'(1 + \eta'\cos\phi')^{-1}] \\ &\quad - \tfrac{1}{2}\sin\phi' \ln(1 + 2\eta'\cos\phi' + \eta'^2)\} \end{aligned} \tag{15}$$

where $\eta' = a^2 \sin\theta_2/rR_2$.

The fluid kinetic energy can be expressed as the sum of the following quantities by using Eq. (6), Gauss' theorem, Green's theorem, and the various properties for Φ:

$$T_p = -\tfrac{1}{2}\rho_s \int_\sigma \Phi_p(\partial\Phi_p/\partial N)\, dS \tag{16}$$

$$T_0 = -\tfrac{1}{2}\rho_s\kappa \int_{s_2} (\partial\Phi_0/\partial N)\, dS \tag{17}$$

$$K = -\tfrac{1}{2}\rho_s \int_\sigma \Phi_v(\partial\Phi_0/\partial N) dS \tag{18}$$

In the three previous expressions, N denotes the surface normal pointing into the fluid. The quantity T_p is the fluid kinetic energy when the vortex is absent, T_0 is the

†The definitions of spherical harmonics are those used in Ref. 8.

fluid kinetic energy when the particle is absent, and $K + T_0$ is the fluid kinetic energy when the particle is at rest. Equations (16) to (18) may be evaluated using the various expressions for the velocity potentials previously determined. One then finds

$$T_p = \tfrac{1}{4}\rho_s \tau \mathbf{v}_p^2 \tag{19}$$

$$T_0 = \tfrac{1}{4}\pi^{-1}\rho_s \kappa^2 L \ln (r_c/\varepsilon) \tag{20}$$

$$K = -\tfrac{3}{4}\rho_s \tau \mathbf{v}_s^2 g(a/r) \tag{21}$$

Here τ is the particle volume $\frac{4}{3}\pi a^3$ and $\mathbf{v}_s$ is the unperturbed fluid velocity (3). The quantity r_c is the radius of the fluid container and L is its length. The function $g(a/r)$ is the correction to large r behavior and its series representation is

$$g(z) = \sum_{l=0}^{\infty} \frac{\Gamma(\frac{1}{2})\Gamma(1+l)}{(2+l)\Gamma(\frac{3}{2}+l)} z^{2l} \tag{22}$$

In Appendix A, Eq. (22) is summed and shown to be

$$g(z) = z^{-4}\{[\arcsin(z)]^2 - 2z(1-z^2)^{1/2}\arcsin(z) + z^2\} \tag{23}$$

As a reminder, the restriction limiting the particle to regions outside the vortex core requires $r \geq a$.

A calculation of the force from Eqs. (5) and (7) is straightforward, although rather tedious; the force is found to be composed of the following components:

$$\mathbf{F}_1 = \tfrac{1}{2}\rho_s \int_\sigma \nabla\Phi \cdot \nabla\Phi \, d\mathbf{S} = -\nabla K + \mathbf{f} \tag{24}$$

$$\mathbf{F}_2 = -\rho_s \int_\sigma (\partial\Phi_p/\partial t)\, d\mathbf{S} = -\tfrac{1}{2}\rho_s \tau \dot{\mathbf{v}}_p \tag{25}$$

$$\mathbf{F}_3 = -\rho_s \int_\sigma (\partial\Phi_v/\partial t)\, d\mathbf{S} = -\mathbf{f} \tag{26}$$

where

$$\mathbf{f} = \tfrac{1}{2}\rho_s \tau \kappa r^{-2}[(\mathbf{v}_p \cdot \hat{\phi})\hat{r} + (\mathbf{v}_p \cdot \hat{r})\hat{\phi}] \tag{27}$$

The total force is thus

$$\mathbf{F} = -\nabla K - \tfrac{1}{2}\rho_s \tau \dot{\mathbf{v}}_p \tag{28}$$

and the equations of motion for the sphere become

$$m^* \dot{\mathbf{v}}_p = -\nabla K \tag{29}$$

where $m^* = m + \frac{1}{2}\rho_s \tau$. The effect of the velocity potential Φ_p is simply to renormalize the particle mass. No forces arise from particle motion other than

inertial force (25). Aside from the inertial effects, the force is the negative gradient of the fluid kinetic energy calculated for a stationary particle.†

An alternate derivation of the equations of motion that avoids the calculation of the force from the pressure can be obtained from a formalism developed in Lamb's book on hydrodynamics.[6] An application of this formalism shows that the equations of motion for the sphere are

$$\frac{d}{dt}\left(\frac{\partial \mathscr{R}}{\partial \mathbf{v}_p}\right) - \frac{\partial \mathscr{R}}{\partial \mathbf{R}} = 0 \tag{30}$$

where $\mathscr{R}$ is the Routhian

$$\mathscr{R} = \tfrac{1}{2}m\mathbf{v}_p^2 + T_p - K - T_0 - \tfrac{3}{2}\rho_s\tau\mathbf{v}_s \cdot \mathbf{v}_p \tag{31}$$

A direct substitution of Eq. (31) into Eq. (30) and the use of some elementary vector identities yield

$$m^*\dot{\mathbf{v}}_p = -\nabla K + \tfrac{3}{2}\rho_s\tau(\partial \mathbf{v}_s/\partial t) - \tfrac{3}{2}\rho_s\tau\mathbf{v}_p \times (\nabla \times \mathbf{v}_s) \tag{32}$$

Since $\partial \mathbf{v}_s/\partial t = \nabla \times \mathbf{v}_s = 0$, Eq. (32) reduces to (29).

The Routhian formalism may be re-expressed in terms of a Hamiltonian formulation by defining the canonical momentum

$$\mathbf{P} = \partial \mathscr{R}/\partial \mathbf{v}_p = m^*\,\mathbf{v}_p - \alpha_1 m^*\mathbf{v}_s \tag{33}$$

and the Hamiltonian

$$H = \mathbf{P} \cdot \mathbf{v}_p - \mathscr{R} = (2m^*)^{-1}(\mathbf{P} + \alpha_1 m^*\mathbf{v}_s)^2 + K + T_0 \tag{34}$$

Here $\alpha_1 = 3(\delta m/m^*)$ and $\delta m = m^* - m$. Equation (30) becomes

$$\dot{\mathbf{P}} = -\partial H/\partial \mathbf{R}, \qquad \dot{\mathbf{R}} = \partial H/\partial \mathbf{P} \tag{35}$$

The first equation in (35) reduces to Eq. (32) while the second is identical to Eq. (33). The momentum $\mathbf{P}$ is the kinematic momentum of the particle $m\mathbf{v}_p$ plus the fluid momentum $\mathbf{I}$ that arises from the presence of the particle, i.e.,

$$\mathbf{I} = \int_\sigma \rho_s\Phi\, d\mathbf{S} = \tfrac{1}{2}\rho_s\tau\mathbf{v}_p - \tfrac{3}{2}\rho_s\tau\mathbf{v}_s \tag{36}$$

It is interesting to note that Hamiltonian Eq. (34) is identical to that of an electron of mass m^* and charge q interacting with an electromagnetic field with scalar potential $q^{-1}(K + T_0)$ and vector potential $-q^{-1}c\alpha_1 m^*\mathbf{v}_s$.[10] Here c is the speed of light.

The preceding model applies when $T = 0$ and only superfluid (density ρ_s) is present. It can be extended to nonzero temperatures where normal fluid (density ρ_n) is present if one is interested in the scattering problem where the superfluid undergoes vortex motion, the normal fluid attempts to remain at rest, and viscosity

†The force on a stationary sphere in the presence of a vortex has previously been calculated by Pratt.[9]

is unimportant. In this case, an examination of Landau's two-fluid equations for liquid He II[11] shows the only effect of the normal fluid is an inertial redefinition of the mass m^*; the effective mass becomes $m + \frac{1}{2}\rho\tau$, where $\rho = \rho_s + \rho_n$ is the total fluid density. This model is an oversimplification of the STK experimental conditions. The normal fluid, viewed as a gas of phonons and rotons, is certainly influenced by the vortex. The normal fluid viscosity induces a drag force (Stokes law) on the sphere that may be neglected if the initial particle velocity is sufficiently small; whether this requirement is met in the STK work is debatable. Also, since the particles are viewed by photographic light reflection, the conversion of superfluid to normal fluid on the particle surface causes an additional drag force[12] that may be important in the STK experiment.

It shall, however, be assumed that the motion of a spherical particle in the presence of a vortex in liquid He II is determined by equations of motion (35) and Hamiltonian

$$H = (2m^*)^{-1}(\mathbf{P} + \alpha_1 m^* \mathbf{v}_s)^2 - \tfrac{1}{2}\alpha_2 m^* \mathbf{v}_s^2 g(a/r) + T_0 \tag{37}$$

where now

$$m^* = m + \tfrac{1}{2}\rho\tau, \qquad \delta m = m^* - m \tag{38}$$

$$\alpha_1 = \alpha_2 = 3(\rho_s/\rho)(\delta m/m^*) \tag{39}$$

and $g(z)$ is given by Eq. (22) or (23). The model is valid for $T = 0$ and may be valid for $T \neq 0$ provided certain experimental conditions are met.

3. CLASSICAL SCATTERING

When the classical scattering problem is studied, it is advantageous, due to the vortex symmetry, to use cylindrical coordinates (r, ϕ, z) (see Section 1). In this case, Hamiltonian (37) is

$$H = (2m^*)^{-1}[p_r^2 + (p_\phi + \alpha_1 m^* \kappa)^2 r^{-2} + p_z^2] - \tfrac{1}{2}\alpha_2 m^* (\kappa/r)^2 g(a/r) + T_0 \tag{40}$$

and equations of motion (35) are

$$\dot{\phi} = \partial H/\partial p_\phi = (m^* r^2)^{-1}(p_\phi + \alpha_1 m^* \kappa) \tag{41}$$

$$\dot{z} = \partial H/\partial p_z = (m^*)^{-1} p_z \tag{42}$$

$$\dot{r} = \partial H/\partial p_r = (m^*)^{-1} p_r \tag{43}$$

$$\dot{p}_\phi = -\partial H/\partial \phi = 0, \qquad p_\phi = \text{constant} \tag{44}$$

$$\dot{p}_z = -\partial H/\partial z = 0, \qquad p_z = \text{constant} \tag{45}$$

$$\dot{p}_r = -\partial H/\partial r = (m^* r^3)^{-1}(p_\phi + \alpha_1 m^* \kappa)^2 + \tfrac{1}{2}\alpha_2 m^* \kappa^2 \, d[r^{-2} g(a/r)]/dr \tag{46}$$

The constant p_z is m^*v_z; the particle has a constant velocity v_z in the z-direction. The constant p_ϕ may be expressed as follows in terms of the impact parameter b and the radial velocity v_r of the particle at infinity (see Fig. 1):

$$p_\phi + m^*\alpha_1\kappa = m^*r^2\dot{\phi} \xrightarrow[r\to\infty]{} m^*bv_r \tag{47}$$

Equation (46) may be integrated. The result is equivalent to H = constant; this is

$$\tfrac{1}{2}m^*v_r^2 = \tfrac{1}{2}m^*\dot{r}^2 + \tfrac{1}{2}m^*v_r^2(b/r)^2 - \tfrac{1}{2}\alpha_2 m^*(\kappa/r)^2 g(a/r) \tag{48}$$

Of obvious importance for comparison to the STK experiment is the orbit equation $\phi(r)$. With the substitution $u = r^{-1}$, one finds from Eqs. (41) and (48) that for the first half of the orbit

$$\phi - \phi_\infty = \int_0^{1/r} b\,du\{1 - u^2[b^2 - \gamma^2 g(au)]\}^{-1/2} \tag{49}$$

where $\gamma^2 = \alpha_2(\kappa/v_r)^2$. An examination of Eq. (49), using the fact that $g(au)$ is an increasing function of u, yields the following qualitative behavior for the orbit: For large enough $|b|$ no loop scattering occurs; as $|b|$ decreases, the particle loops once, twice, etc.; as $|b|$ further decreases, a value is reached below which $\dot{r}$ always increases and the particle spirals into the center of the vortex. It is in this latter case that the detailed nature of the vortex core would become important, and the simple model presented here would break down. One usually assumes that capture occurs for those values of $|b|$ that lead to spiral orbiting.

The other interesting quantity for STK comparison is the time of flight T_{fi} between orbit points (i, f). Since $dt = d\phi/\dot{\phi} = dr/\dot{r}$, one immediately has for the first half of the orbit

$$v_r T_{fi} = \int_{\phi_i}^{\phi_f} d\phi b^{-1} r^2(\phi) = \int_{1/r_i}^{1/r_f} u^{-2}\,du\,\{1 - u^2[b^2 - \gamma^2 g(au)]\}^{-1/2} \tag{50}$$

The flight time is also related to the corresponding area A_{fi} swept out by the radius vector as follows:

$$A_{fi} = \int_{t_i}^{t_f} \tfrac{1}{2}r^2\dot{\phi}\,dt = \tfrac{1}{2}bv_r T_{fi} \tag{51}$$

Consider the case where the particle radius is small compared to the closest distance the particle approaches the vortex axis; this condition corresponds to the experimental situation of STK. In this case, $g(au)$ equals 1 and Eqs. (49) and (50) yield

$$\phi - \phi_\infty = (b/r_a)\arcsin(r_a/r) \tag{52}$$

$$r_a/r = \sin[(r_a/b)(\phi - \phi_\infty)] \tag{53}$$

$$v_r T_{fi} = -r_a \cot[(r_a/b)(\phi - \phi_\infty)]\Big|_{\phi_i}^{\phi_f} \tag{54}$$

The distance of closest approach is $r_a = (b^2 - \gamma^2)^{1/2}$.

If first-order corrections in (a/r_a) are included, i.e., $g(au) = 1 + (4/9)(au)^2$, Eqs. (49) and (50) yield

$$\phi - \phi_\infty = (b/r_a)(\xi u_2^2)^{-1/2} F[\arcsin(u/u_1); u_1/u_2] \tag{55}$$

$$u/u_1 = sn[(r_a/b)(\xi u_2^2)^{1/2}(\phi - \phi_\infty)] \tag{56}$$

$$v_r T_{fi} = -r_a(\xi u_2^2)^{-1/2} u_1^{-2}[F(\zeta, u_1/u_2) - E(\zeta, u_1/u_2) + (u_2/u)(u_1^2 - u^2)^{1/2}(u_2^2 - u^2)^{-1/2}]\Big|_{u_i}^{u_f} \tag{57}$$

where

$$r_a = (b^2 - \gamma^2)^{1/2}, \qquad r_b^2 = \tfrac{2}{3}\gamma a, \qquad u = r_a/r$$

$$\xi = (r_a/r_b)^4, \qquad 2\xi u_{1,2}^2 = 1 \mp (1 - 4\xi)^{1/2}$$

$$\zeta = \arcsin[(u_2/u_1)(u_1^2 - u^2)^{1/2}(u_2^2 - u^2)^{-1/2}] \tag{58}$$

The function $F(\phi, k)$ is an elliptic integral of the first kind, $E(\phi, k)$ is an elliptic integral of the second kind, and $sn(u)$ is the Jacobian sine-amplitude function.[13]

4. RESULTS FOR ONE-LOOP ORBITS

In discussing results for one-loop orbits, it is convenient to orient the coordinate system so that the angle of closest approach occurs at $\frac{3}{2}\pi$. If the orbits are observed by photographic techniques, the measurable quantities are the width of the orbit d, the orbit length D, the orbit time T and related area A, the incident angle ϕ_∞, and possibly the radial velocity v_r of the particle at infinity (see Fig. 1). Results for the simplest case where $g(au) = 1$ are as follows:

$$r(\phi) = r_a \csc[\tfrac{1}{2}\pi(\phi - \phi_\infty)/\phi_f], \qquad \phi_f = \tfrac{3}{2}\pi - \phi_\infty \tag{59}$$

$$r_a = \gamma[4\pi^{-2}\phi_f^2 - 1]^{-1/2} \tag{60}$$

$$v_r T = 2r_a \cot[\tfrac{1}{2}\pi(\phi_i/\phi_f)], \qquad \phi_i = \tfrac{1}{2}\pi - \phi_\infty \tag{61}$$

$$A = \pi^{-1}\phi_f r_a v_r T \tag{62}$$

$$D = r_a\{1 + \csc[\tfrac{1}{2}\pi(\phi_i/\phi_f)]\} \tag{63}$$

$$d = 2r(\phi_d)\cos\phi_d \approx 2.36 r_a(1 + 0.087\phi_\infty), \qquad |\phi_\infty| \ll 1 \tag{64}$$

Here ϕ_d satisfies the equation

$$\phi_f \tan\phi_d = -\tfrac{1}{2}\pi \cot[\tfrac{1}{2}\pi(\phi_d - \phi_\infty)/\phi_f] \tag{65}$$

For $|\phi_\infty| \ll 1$, $\phi_d \approx 2.919 - 0.124\phi_\infty$.

The values for the quantization integer n can then be found from the relations

$$n = \left(\frac{\pi^2 D^2}{\kappa' T}\right)\frac{1}{\lambda_1} = \left(\frac{\pi D v_r}{\kappa'}\right)\frac{1}{\lambda_2} = \left(\frac{v_r^2 T}{\kappa'}\right)\frac{1}{\lambda_3} = \left(\frac{4\pi A}{\kappa' T}\right)\frac{1}{\lambda_4} \tag{66}$$

where

$$\lambda_1 = \tfrac{1}{4}\pi\beta(\alpha_2)^{1/2}(1 + \csc\Phi)^2 \tan\Phi$$
$$\lambda_2 = \tfrac{1}{2}\beta(\alpha_2)^{1/2}(1 + \csc\Phi)$$
$$\lambda_3 = \pi^{-1}\beta(\alpha_2)^{1/2}\cot\Phi$$
$$\lambda_4 = 2\pi^{-1}\phi_f\beta(\alpha_2)^{1/2} \tag{67}$$

and

$$\Phi = \tfrac{1}{2}\pi(\phi_i/\phi_f), \qquad \beta = [4\pi^{-2}\phi_f^2 - 1]^{-1/2}, \qquad \kappa' = h/m_4 \tag{68}$$

The quantities in parentheses in Eq. (66) are the values of n that are obtained with the STK assumption. The λ's are numerical functions of the orbit shape and α_2. It is not surprising that Eq. (66) is similar to the STK expressions—dimensional analysis would yield the same results.

The constant α_2 is defined as

$$\alpha_2 = 3(\rho_s/\rho)(\delta m/m^*) = \tfrac{3}{2}\rho_s(\rho_p + \tfrac{1}{2}\rho)^{-1} \tag{69}$$

where ρ_p is the particle density. In the STK experiment, the particle densities were adjusted to equal the density of helium so that gravitational effects were negligible. In this case, $\rho_p = \rho$ and $\alpha_2 = \rho_s/\rho$. Thus α_2 is somewhat temperature-dependent ($0.4 < \alpha_2 < 0.8$) in the experimental temperature range between 1.4°K and 2.0°K.

Various orbits are plotted in Fig. 3 for $g(au) = 1$. The special results for $\phi_\infty = 0$ are summarized in Fig. 4. Figure 5 shows the effect of attempting to determine the quantization integer n from a plot of $n_{\text{exp}}/\lambda_1(0)$, where $n_{\text{exp}} = (\pi^2 D^2/\kappa' T)$ is the quantization integer predicted by STK and $\lambda_1(0)$ is the value of λ_1 at $\phi_\infty = 0$ [$\lambda_1(0) = (3\pi/16)(6\alpha_2)^{1/2} \approx 1$]. Since n is given by Eq. (66), one finds widths produced around integer values of $n_{\text{exp}}/\lambda_1(0)$ in Fig. 5; the sizes of the widths depend on the range of orbits (values of ϕ_∞) observed. It would thus be difficult to determine n from a plot of $n_{\text{exp}}/\lambda_1(0)$. Consequently, if the model considered in this article is correct, the STK data ($n = n_{\text{exp}}$) do not give the correct values for n and should be re-analyzed using Eq. (66) and taking the shape of particle orbits into account.

An order-of-magnitude estimate for the probability of single-loop scattering can be obtained as follows. Assume there is one vortex at the center of a square of area L^2 and that a uniform distribution of particles with velocity v_r is incident upon the vortex from infinity. The probability for single-loop scattering is then

$$P_L = 2(b_2 - b_1)/L \tag{70}$$

where $b = 2\phi_f\gamma\beta\pi^{-1}$, and b_1 and b_2 are the limiting values of $b > 0$ for which one-loop scattering is observed. The factor of two occurs because clockwise orbits are as equally probable as counterclockwise orbits. Now,

$$P_L = 2\gamma(c_2 - c_1)/L = \tfrac{4}{3}2^{1/2}(c_2 - c_1)(D_L/L) \tag{71}$$

where D_L is the orbit length for $\phi_\infty = 0$ and $c = b/\gamma$. Taking $D_L \approx 0.005$ cm, $c_2 - c_1 \approx 0.05$ (loops observed for $\phi_\infty = \pm\frac{1}{3}\pi$), and $L \approx 0.04$ cm (approximate

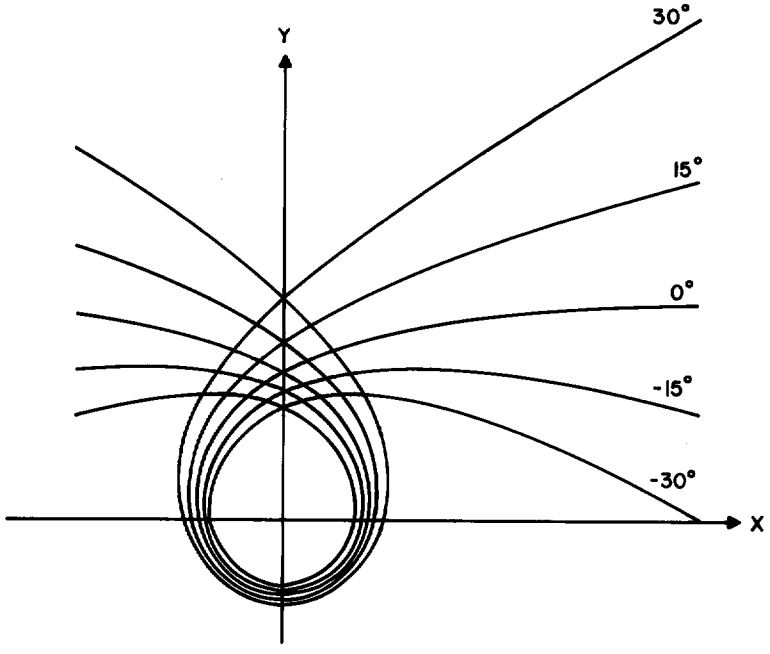

Fig. 3. Particle trajectories $r(\phi)/\gamma$ for various values of ϕ_∞; only the simplest case where the particle size is small compared to the distance of closest approach [$g(au) = 1$] is given.

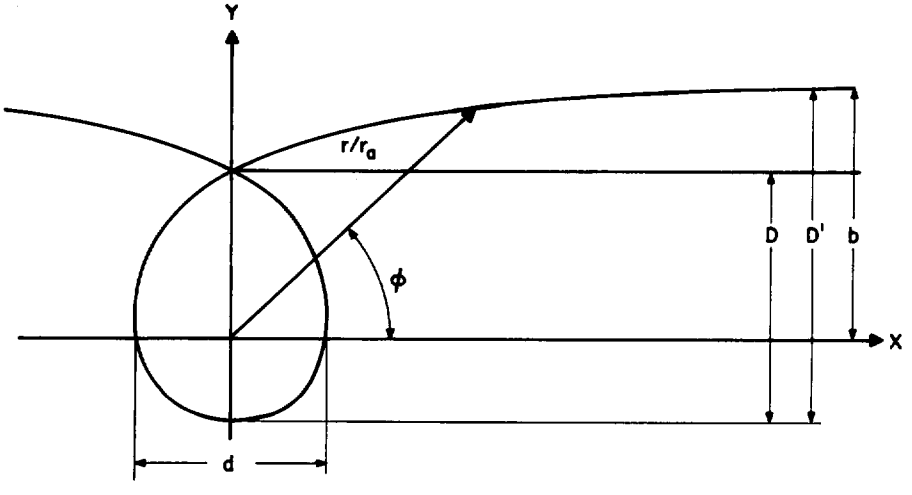

Fig. 4. Results for loop behavior when $\phi_\infty = 0$ and $g(au) = 1$. The orbit equation is $r = r_a \csc(\frac{1}{3}\phi)$, where $r_a = (8)^{-1/2}\gamma$. The orbit parameters are $d = 2.36r_a$, $D = b = 3r_a$, $D' = 4r_a$, $A = 3(3)^{1/2}r_a^2$, and $v_r T = 2(3)^{1/2}r_a$. The λ_i's of Eq. (66) are $\lambda_1 = (3\pi/16)(6\alpha_2)^{1/2}$, $\lambda_2 = (3/8)(2\alpha_2)^{1/2}$, $\lambda_3 = (1/4\pi)(6\alpha_2)^{1/2}$, and $\lambda_4 = (3/4)(2\alpha_2)^{1/2}$.

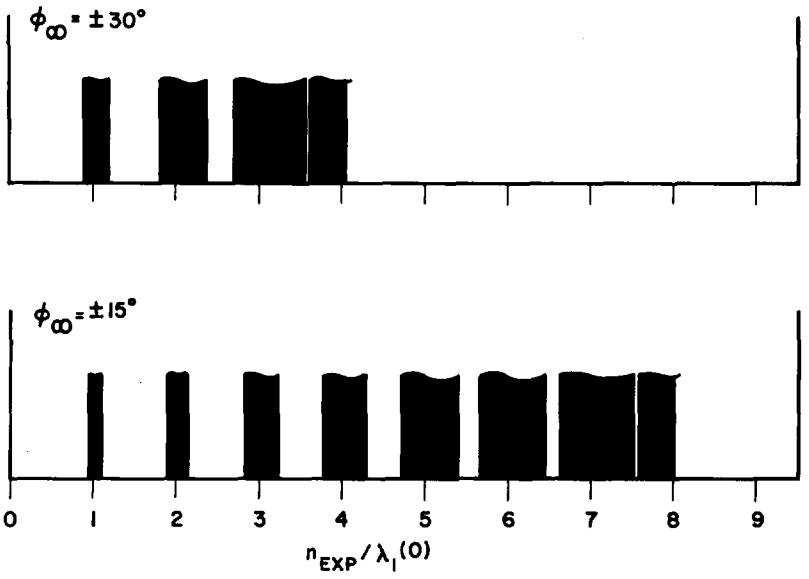

Fig. 5. Theoretical values of $n_{exp}/\lambda_1(0)$ for the case $g(au) = 1$ when the limiting orbits observed are $\phi_\infty = \pm 30°$ and $\phi_\infty = \pm 15°$. Here $n_{exp} = (\pi^2 D^2/\kappa' T)$ and $\lambda_1(0) = (3\pi/16)(6\alpha_2)^{1/2}$.

length of a square area containing a single vortex in a cylinder rotating at 0.05 rev/sec), one finds that $P_L \approx 1/85$. The experimental probability is about 1/1000. The discrepancy is probably due to an underestimation of L; the experimental vortex density may have been much smaller than that corresponding to a cylinder rotating at 0.05 rev/sec.

STK also found that if the experiment was performed in a rotating cylinder, the number of clockwise orbits N_c was not equal to the number of counterclockwise orbits N_{cc}. Indeed

$$(N_c - N_{cc})/(N_c + N_{cc}) \approx \pm 0.5 \tag{72}$$

where the upper sign holds for clockwise rotations of the cylinder and the lower sign for counterclockwise rotations. If the fluid in the cylinder were at rest and the vortices present uniformly distributed, the model given in this article would predict that $N_c = N_{cc}$. A possible explanation for the difference in N_c and N_{cc} in the case of rotation can be obtained by noting that the probability for loop scattering is inversely proportional to the particle velocity at infinity. If one assumes the particles are initially at rest in the container and that the vortices are moving with velocity $v_r = \Omega r$ (here Ω is the angular velocity of the cylinder and r is the radial distance from the center of the cylinder), one would expect the ratio in Eq. (72) to have the sign indicated by experiment due to the r dependence of v_r. A very crude calculation yields a value of ± 0.36 for Eq. (72).

Finally, the following is a summary of the results of loop scattering when first-order corrections in (a/r_a) are included:

$$r(\phi) = r^0(\phi)[1 - \tfrac{1}{2}\xi - \tfrac{1}{16}\xi(1 + \csc\Phi_i \sin 3\Phi_i) + \xi\Delta] \tag{73}$$

$$r_a = r_a^0[1 + \xi\Delta] \tag{74}$$

$$v_r T = v_r T^0[1 - \tfrac{3}{4}\xi + \tfrac{1}{2}\xi(\tfrac{1}{2}\pi - \Phi)\tan\Phi + \xi\Delta] \tag{75}$$

$$A = A^0[1 - \tfrac{3}{2}\xi + \tfrac{1}{2}\xi(\tfrac{1}{2}\pi - \Phi)\tan\Phi + 2\xi\Delta] \tag{76}$$

$$D = D^0[1 - \tfrac{1}{2}\xi - \tfrac{1}{16}\xi(1 + \sin\Phi)^{-1}(1 + \csc\Phi \sin 3\Phi) + \xi\Delta] \tag{77}$$

Here $r^0(\phi)$, r_a^0, T^0, A^0, and D^0 are the corresponding quantities given in Eqs. (59) to (63). Also

$$\xi = (4/9)(a/\gamma)^2\beta^{-4}, \qquad \beta = (4\pi^{-2}\phi_f^2 - 1)^{-1/2}, \qquad \Delta = 3\pi^{-2}\phi_f^2\beta^2$$

$$\phi_i = \tfrac{1}{2}\pi - \phi_\infty, \qquad \phi_f = \tfrac{3}{2}\pi - \phi_\infty$$

$$\Phi_i = \tfrac{1}{2}\pi(\phi - \phi_\infty)/\phi_f, \qquad \Phi = \tfrac{1}{2}\pi(\phi_i/\phi_f) \tag{78}$$

The relations in Eq. (66) are still valid provided the λ_i's are replaced by $\lambda_{i0}\lambda_{ii}$, where λ_{i0}'s are the values in Eq. (67) and

$$\lambda_{11} = 1 - \tfrac{1}{4}\xi - \tfrac{1}{8}\xi(1 + \sin\Phi)^{-1}(1 + \csc\Phi \sin 3\Phi) - \tfrac{1}{2}\xi(\tfrac{1}{2}\pi - \Phi)\tan\Phi + \xi\Delta$$

$$\lambda_{21} = 1 - \tfrac{1}{2}\xi - \tfrac{1}{16}\xi(1 + \sin\Phi)^{-1}(1 + \csc\Phi \sin 3\Phi) + \xi\Delta$$

$$\lambda_{31} = 1 - \tfrac{3}{4}\xi + \tfrac{1}{2}\xi(\tfrac{1}{2}\pi - \Phi)\tan\Phi + \xi\Delta$$

$$\lambda_{41} = 1 - \tfrac{3}{4}\xi + \xi\Delta \tag{79}$$

The parameter ξ is very small in the STK experiment,† and consequently first-order corrections in ξ may be neglected for experimental interpretation.

5. TRANSPORT CROSS SECTIONS

In this section, a classical analogue of an Iordanskii force[7] will be discussed; the discussion will require the calculation of certain cross sections. For convenience, the coordinate system will be oriented so that ϕ_∞ is zero, and only the case $g(au) = 1$ will be considered. The multiloop scattering complicates the calculation of cross sections since many different values of b can contribute to the same scattering angle $0 \le \chi < 2\pi$. If χ is defined counterclockwise from the incident direction (see Fig. 1), it is related to the angle of closest approach ϕ_n (n is a nonzero integer) by

$$\chi = 2\phi_n - (2n - 1)\pi, \qquad n \neq 0, \qquad |b| > \gamma \tag{80}$$

Since $\phi_n = \tfrac{1}{2}\pi(b/r_a)$ and $r_a = (b^2 - \gamma^2)^{1/2}$, a particle is scattered between χ and $\chi + d\chi$ whenever b has a value between b_n and $b_n + db_n$. Here

$$b_n = \gamma[\chi + (2n - 1)\pi]\{[\chi + (2n - 1)\pi]^2 - \pi^2\}^{-1/2}, \qquad n \neq 0 \tag{81}$$

†When $\phi_\infty = 0$, one finds $\xi = 8(D_p/D_L)^2$. Here D_p is the particle diameter and D_L is the length of the orbit.

Consequently the differential cross section is

$$d\sigma/d\chi = \sum_{n\neq 0} |db_n/d\chi| = \sum_{n\neq 0} \gamma\pi^2\{[\chi + (2n-1)\pi]^2 - \pi^2\}^{-3/2} \tag{82}$$

The experimental quantities of interest are usually the frictional force per unit length for a rectilinear vortex with translational velocity $-\mathbf{U}$, and the corresponding momentum transport cross sections.[3] In particular,

$$F_c = -(m^*)^{-1}\pi U \int_0^\infty p^4\, dp \int_{-\infty}^{\infty} dp_z[\partial f(E)/\partial E]\sigma_c(p) \tag{83}$$

$$\sigma_c(p) = \int_0^{2\pi} d\chi(1 - e^{i\chi})(d\sigma/d\chi) \tag{84}$$

Here the real part of F_c is the force in the $\mathbf{U}$ direction while the imaginary part is the force in the $\boldsymbol{\kappa} \times \mathbf{U}$ direction. The real part of σ_c is the forward transport cross section and the imaginary part is the transverse. The quantity p is the radial momentum and E is the energy $(2m^*)^{-1}(p^2 + p_z^2)$. The function

$$f(E) = (2\pi m^* k_B T)^{-3/2} n_p \exp(-E/k_B T) \tag{85}$$

is the equilibrium distribution for a classical gas of particles with zero drift velocity, normalized to n_p particles per unit volume. Here T is the temperature and k_B is Boltzmann's constant.

With differential cross section (82), Eqs. (83) and (84) may be evaluated to give[3]

$$\sigma_c = \gamma\pi^2 Y_1(\pi) \tag{86}$$

$$F_c = \pi^2 U n_p m^* \kappa(\alpha_2)^{1/2} Y_1(\pi) \tag{87}$$

where $Y_1(\pi)$ is the Neumann function of order one and argument π. Cross section (86) includes a contribution 2γ from capture.

Iordanskii found that an additional transverse frictional force

$$F_c' = -i\rho_n \kappa U \tag{88}$$

was present in quasiparticle-vortex scattering (phonons and rotons) when the cross sections were calculated by introducing a cutoff for the vortex velocity at radial distances greater than some large r_0. The quantity ρ_n is the quasiparticle density. If such a cutoff is introduced in the present problem, an additional transverse cross section

$$\sigma_c' = i\alpha_1 m^*(\kappa/p) \tag{89}$$

arises from the long-range nature of the force (see Appendix B). Substitution of Eq. (89) into Eq. (83) yields the transverse force

$$F_c' = i\alpha_1 \kappa \rho_n U \tag{90}$$

where $\rho_n = m^* n_p$. In the Iordanskii problem, the interaction is such that $\alpha_1 = 1$; in this case, Eq. (90) is the negative of Eq. (88).

Thus, if one is interested in the scattering problem for an infinite medium, but can only calculate the cross sections by introducing a cutoff, a quantity equal to the negative of Eq. (90) must be added to the frictional force in order to obtain the correct results. This appears to be the origin of the Iordanskii force (88).

6. CONCLUSION

A simple classical model for the scattering of a small particle by a rectilinear vortex in liquid He II has been presented. The model appears to explain some of the features of the STK experiment such as orbit shapes and loop probabilities. However, verification of the theory would require a re-analysis of the experimental data. Relations of the type given in Eq. (66) that critically depend on the shape of the orbit (value of ϕ_∞) could be used to determine the quantization integer n. The use of Eq. (1) for a determination of n, instead of Eq. (66), may partially be the reason the $n = \frac{1}{2}$ value was observed. However, caution should be used in any interpretation since the theoretical model is an oversimplification of the experimental situation. In particular, it was assumed the normal fluid viscosity vanished, no conversion of superfluid to normal fluid occurred on the particle surface, and the normal fluid attempted to remain at rest while the superfluid underwent vortex flow. The latter assumption is probably not justified for the case where fluid motion arises from heat currents; it was with this type of fluid flow that the value of $n = \frac{1}{2}$ was found. The former assumptions may or may not be valid. Their importance could be reduced by repeating the STK experiment with smaller particles at lower temperatures.

APPENDIX A

The series (22) for $g(z)$

$$g(z) = \sum_{l=0}^{\infty} \frac{\Gamma(\frac{1}{2})\Gamma(1+l)}{(2+l)\Gamma(\frac{3}{2}+l)} z^{2l} \tag{A1}$$

is related to the hypergeometric function (Ref. 13, Sec. 9.10)

$$F(1, 1, \tfrac{3}{2}; x) = \sum_{l=0}^{\infty} \frac{\Gamma(\frac{3}{2})\Gamma(1+l)}{\Gamma(\frac{3}{2}+l)} x^l \tag{A2}$$

by

$$g(z) = 2z^{-4} \int_0^{z^2} xF(1, 1, \tfrac{3}{2}; x)\, dx \tag{A3}$$

However, since $F(1, 1, \frac{3}{2}; \sin^2 y) = 2y \csc(2y)$ (Ref. 13, Eq. 9.121(14)), one has that

$$g(z) = 4z^{-4} \int_0^{y_0} y \sin^2 y\, dy = z^{-4}[y_0^2 - 2z(1 - z^2)^{1/2} y_0 + z^2] \tag{A4}$$

where $y_0 = \arcsin(z)$.

APPENDIX B

Consider the case where the superfluid velocity $\mathbf{v}_s$ vanishes for radial distances greater than $r_0 \gg \gamma$. The Hamiltonian formulation of Section 2 yields the relevant equations

$$p_z = m^* v_z, v_z = \text{constant} \tag{B1}$$

$$p_\phi = m^* b v_r, v_r = \text{radial velocity at infinity} \tag{B2}$$

$$\tfrac{1}{2}m^* v_r^2 = \tfrac{1}{2}m^* \dot{r}^2 + \tfrac{1}{2}m^*[v_r(b + w\Theta)/r]^2 - \tfrac{1}{2}\alpha_2 m^*(\kappa/r)^2 \Theta g(a/r) \tag{B3}$$

$$\phi = \int_0^{1/r} du(b + w\Theta)\{1 - u^2[(b + w\Theta)^2 - \gamma^2 g(au)]\}^{-1/2} \tag{B4}$$

where $w = \alpha_1(\kappa/v_r)$ and $\phi_\infty = 0$. The quantity Θ is the step function

$$\Theta(r_0 - r) = \begin{cases} 1, r_0 > r \\ 0, r_0 < r \end{cases} \tag{B5}$$

With the approximation $g(au) = 1$, one then finds that the angle of closest approach is

$$\begin{aligned} &\phi_n = \tfrac{1}{2}\pi b(b^2 - \gamma^2)^{-1/2}, && |b| \geq r_0 \\ &\phi_n = \tfrac{1}{2}\pi b'(b'^2 - \gamma^2)^{-1/2} + \Delta\phi_n, && \gamma < |b| < r_0, \quad \gamma < |b'|, \quad (b'^2 - \gamma^2)^{1/2} < r_0 \end{aligned} \tag{B6}$$

where

$$b' = b + w \tag{B7}$$

$$\begin{aligned} \Delta\phi_n = {} & b(b^2 - \gamma^2)^{-1/2} \arcsin[(b^2 - \gamma^2)^{1/2}/r_0] \\ & - b'(b'^2 - \gamma^2)^{-1/2} \arcsin[(b'^2 - \gamma^2)^{1/2}/r_0] \end{aligned} \tag{B8}$$

Capture is assumed to occur for all other values of b.

The transport cross section (84) can also be expressed in the form

$$\sigma_c = \int db[1 - e^{i(2\phi_n + \pi)}] \tag{B9}$$

where the integration is carried out over those values of b where capture does not occur. Consequently, to lowest order in $1/r_0$,

$$\sigma_c = (\sigma_c)_0 + \int db(-2i\Delta\phi_n)_{\gamma=0} \tag{B10}$$

The cross section $(\sigma_c)_0$ is that which would be calculated without cutoff. The remainder is the cross section due to cutoff, i.e.,

$$\begin{aligned} \sigma_c' &= -2i \int_{-r_0}^{r_0 - w} [\arcsin(b/r_0) - \arcsin(b'/r_0)]\, db \\ &= 2\pi i w + 0(r_0^{-1/2}) \end{aligned} \tag{B11}$$

and is the result (89) quoted in Section 5.

REFERENCES

1. W. A. Steyert, R. D. Taylor, and T. A. Kitchens, *Phys. Rev. Letters* **15**, 546 (1965).
2. W. Thomson, *Phil. Mag* **45**(4), 332 (1873).
3. A. L. Fetter, *Phys. Rev.* **151**, 112 (1966).
4. L. M. Milne-Thomson, *Theoretical Hydrodynamics* (Macmillan Co., New York, 1968), 5th ed., Sec. 3.60.
5. R. J. Donnelly, in *Experimental Superfluidity* (University of Chicago Press, Chicago, 1967), p. 182.
6. H. Lamb, *Hydrodynamics* (Dover Publications, New York, 1945), 6th ed., Secs. 139–141.
7. S. V. Iordanskii, *Zh. Eksperim. i Teor. Fiz.* **49**, 225 (1965) [English transl.: *Soviet Phys.—JETP* **22**, 160 (1966)].
8. J. D. Jackson, *Classical Electrodynamics* (John Wiley & Sons, Inc., New York, 1962).
9. W. P. Pratt, Jr., Ph.D. thesis, University of Minnesota, 1967 (unpublished).
10. H. Goldstein, *Classical Mechanics* (Addison-Wesley Publishing Co., Inc., Reading, Mass., 1950), Sec. 7.3.
11. Reference 5, Sec. 16.
12. R. Penny and T. K. Hunt, *Phys. Rev.* **169**, 228 (1968).
13. I. S. Gradshteyn and I. M. Ryzhik, *Table of Integrals, Series, and Products* (Academic Press, New York, 1965), 4th ed., Sec. 8.1.